Frontiers in Bioscience Landmark

Front. Biosci. (Landmark Ed) **2026**; 31(11): 52984
https://doi.org/10.31083/FBL52984

Original Research

Mechanisms Underlying CD109-Mediated Progression of Gastric Adenocarcinoma via the PI3K/AKT Pathway

Yi Yang[1,2,†], Yuliang Wei[3,†], Chaowei Zhu[1,4], Ying Yan[5], Yuxiang Fu[1,4], Keli Zhong[1,4,*]

[1]Department of Gastrointestinal Surgery, The Second Clinical Medical College, Jinan University (Shenzhen People's Hospital), 518020 Shenzhen, Guangdong, China
[2]Post-doctoral Scientific Research Station of Basic Medicine, Jinan University, 510632 Guangzhou, Guangdong, China
[3]Department of Hepatobiliary Surgery, The Fifth Affiliated Hospital of Jinan University, 517000 Heyuan, Guangdong, China
[4]Department of Gastrointestinal Surgery, The First Affiliated Hospital, Southern University of Science and Technology, 518020 Shenzhen, Guangdong, China
[5]The School of Pharmaceutical Sciences, Guangzhou University of Chinese Medicine, 510006 Guangzhou, Guangdong, China
*Correspondence: zhongkeli@126.com (Keli Zhong)
[†]These authors contributed equally.

Academic Editor: Amancio Carnero Moya
Submitted: 16 April 2026 Revised: 17 August 2026 Accepted: 2 September 2026 Published: 4 November 2026

Abstract

Introduction: Stomach adenocarcinoma (STAD) continues to be one of the leading causes of cancer-related mortality globally. While immune checkpoint blockade therapy has shown efficacy in several malignancies, its overall response rate in STAD patients requires further improvement. This study identifies CD109 as a critical player in suppressing anti-tumor immunity in STAD. **Method:** Gene expression data and corresponding clinical information were obtained from public databases. Survival analysis was employed to assess patient prognosis. Enrichment analysis and single-cell sequencing data were utilized to evaluate the potential efficacy of immunotherapy, and findings from bioinformatics were validated through *in vitro* experiments. **Results:** Analyses indicated that CD109 expression increased substantially in STAD tissues relative to surrounding normal tissues, and its elevated expression functioned as an independent predictive indicator for adverse patient outcomes. *In vitro* functional studies showed that the knockdown of CD109 significantly inhibited the proliferation, invasion, and migration of gastric cancer cells. Mechanistic investigations suggested that changes induced by CD109 may be associated with alterations in epithelial-mesenchymal transition (EMT) markers. Additionally, CD109 expression levels exhibited strong associations with the infiltration of diverse immune cells (e.g., $CD8^+$ T cells, M2 macrophages) in the STAD tumor microenvironment and were linked to the expression of several immune checkpoint markers. This indicates its potential as a biomarker for assessing immune microenvironment status and predicting response to immunotherapy. **Conclusion:** Our results indicate that CD109 has a significant oncogenic function in STAD. The expression level shows potential as a predictive biomarker that warrants further investigation in immunotherapy-treated cohorts. Targeting CD109 may therefore represent a novel and effective therapeutic strategy for gastric adenocarcinoma.

Keywords: adenocarcinoma; CD109 protein; tumor microenvironment; immune checkpoints

1. Introduction

Stomach adenocarcinoma (STAD) continues to be a significant public health concern globally, characterized by consistently elevated incidence and fatality rates [1]. Adenocarcinoma constitutes the predominant histological type of gastric malignancies. The onset and advancement of gastric adenocarcinoma are closely linked to several recognized risk factors, including Helicobacter pylori infection, obesity, and gastroesophageal reflux syndrome [2]. Surgical resection can achieve favorable outcomes in early-stage STAD; however, early disease is frequently asymptomatic, and endoscopic screening is not widely implemented. As a result, a substantial proportion of patients present with advanced-stage tumors and lose the opportunity for curative surgery [3,4]. Although systemic chemotherapy, molecularly targeted agents, and immunotherapies have improved the management of advanced STAD, long-term survival and overall prognosis remain far from satisfactory. Therefore, improving early detection, refining diagnostic strategies, and optimizing treatment regimens are pressing clinical needs in STAD [5].

The continual enrichment and refinement of large-scale genomic resources, such as The Cancer Genome Atlas (TCGA), have made it possible to profile differentially expressed genes in tumors using bioinformatics approaches [6,7]. Systematic interrogation of these genes as potential diagnostic and prognostic biomarkers, together with functional assessment of their roles in key oncogenic processes (e.g., proliferation, migration), may yield valuable clues for disease diagnosis, therapeutic decision-making, and prognosis stratification [8]. Nevertheless, biomarkers proposed

Copyright: © 2026 The Author(s). Published by IMR Press.
This is an open access article under the CC BY 4.0 license.

Publisher's Note: IMR Press stays neutral with regard to jurisdictional claims in published maps and institutional affiliations.

solely on the basis of computational prediction often suffer from limited specificity and sensitivity and thus require rigorous experimental confirmation. Consequently, the integration of bioinformatics analysis with molecular and cellular experiments to identify and validate robust biomarkers has become a central theme in gastric cancer research.

Immunotherapy has significantly transformed the treatment paradigm for numerous malignancies and is becoming acknowledged as an essential approach in gastric cancer management. In STAD, currently explored immunotherapeutic strategies encompass immune checkpoint inhibitors (ICIs), chimeric antigen receptor T-cell (CAR-T) therapies, and cancer vaccines, among which ICIs are the most extensively investigated and widely adopted in clinical practice [9]. ICIs exert their effects by blocking inhibitory checkpoint molecules or their ligands expressed on immune cells (such as T cells) or tumor cells, thereby restoring antitumor immune activity and facilitating the elimination of malignant cells [10,11]. However, most clinical trials of ICIs in gastric cancer have enrolled heterogeneous and relatively unselected patient populations, partly to ensure adequate accrual and partly due to the paucity of validated predictive biomarkers that can identify likely responders. Thus, key challenges in this field include improving patient stratification for immunotherapy, defining novel immune-related targets, and establishing rational combination strategies among the expanding armamentarium of treatment options.

Leukocyte differentiation antigen 109 (CD109) is a recently identified cell-surface molecule belonging to the family of glycosylphosphatidylinositol (GPI)–anchored glycoproteins [12]. CD109 has been demonstrated to influence cell proliferation and differentiation mostly by inhibiting transforming growth factor-β (TGF-β) signaling [13,14]. In addition, it has been implicated in the Janus kinase–signal transducer and activator of transcription (JAK-STAT) and epidermal growth factor receptor (EGFR) pathways [15]. Accumulating data indicate that CD109 participates in the pathogenesis of multiple malignancies [16]. The overexpression of CD109 has been documented in multiple tumor cell lines and diverse solid tumor tissues, indicating its potential as a diagnostic biomarker and a candidate for therapeutic targeting [17]. However, the precise biological roles of CD109 in gastric adenocarcinoma and the mechanisms by which it facilitates tumor progression are still mainly ambiguous and necessitate thorough investigation through integrated bioinformatics and experimental research.

This study integrates analyses of public databases, clinical specimen assessments, and *in vitro* functional assays to systematically elucidate the contribution of CD109 in STAD. Our findings elucidate the role of CD109 in the evolution of STAD, define its prognostic relevance, and disclose its correlation with the formation of an immunological tumor microenvironment.

2. Materials and Methods

2.1 Acquisition and Analysis of STAD Transcriptomic Data

RNA-sequencing data and corresponding clinical information for STAD and matched normal gastric tissues were acquired from The Cancer Genome Atlas (TCGA) portal (https://portal.gdc.cancer.gov/) and Gene Expression Omnibus (GEO) database (https://www.ncbi.nlm.nih.gov/geo/) [18]. Normal samples were obtained from the GTEx project (stomach, n = 391). The expression matrix was processed and normalized, and CD109 expression profiles were extracted and analyzed using the "limma" (version 3.69.2) package in R. The limma package was developed and maintained by Gordon Smyth at the Walter and Eliza Hall Institute of Medical Research (WEHI), Parkville, Victoria, Australia. The package is part of the Bioconductor project. The differential gene expression for CD109 between tumor and non-tumor specimens was assessed, and the Wilcoxon rank-sum test was utilized to compare expression levels in STAD and normal stomach tissues.

2.2 Single-Cell RNA Sequencing Data Analysis

Single-cell RNA sequencing (scRNA-seq) data from gastric cancer tissues were obtained from the Gene Expression Omnibus (GEO) database (GSE134520). Data preprocessing and quality control were performed according to standard procedures. The scRNA-seq data were processed and analyzed using the R software package "Seurat". First, cells were quality filtered based on the following criteria: (a) the number of genes detected per cell (nFeature_RNA) was greater than 200 and less than 5000; (b) the percentage of mitochondrial genes (percent.mt) was less than 20%; and (c) the UMI count per cell was greater than 500. Low-quality cells and potential doublets were excluded based on the above criteria. After data filtering, the expression matrix was standardized using the "LogNormalize" method. Subsequently, linear dimensionality reduction was performed using principal component analysis (PCA), and the top 30 principal components were selected for subsequent analysis. Based on the PCA results, cell clustering was performed using the Louvain or Leiden algorithm optimized based on the shared nearest neighbor (SNN) module. Cell type annotation referenced known cell type marker genes and was performed using SingleR or manual annotation methods. Differentially expressed genes were screened using the "FindAllMarkers" function, with the selection criteria being $|\log_2 FC| > 0.25$ and an adjusted p-value < 0.05.

2.3 Clinical Patients and Samples and Immunohistochemistry (IHC) Staining

A total of 120 pairs of primary STAD tissues and their corresponding adjacent non-tumorous gastric mucosa were procured from individuals who received curative gastrointestinal surgery at the First Affiliated Hospital of Jinan University. The diagnosis of STAD was confirmed by postoperative histopathological examination. Individuals who had

received any form of neoadjuvant treatment before surgery were not included. Resected specimens were preserved in paraformaldehyde, transformed into wax blocks, and sectioned serially. Immunohistochemical detection of CD109 was carried out using a specific anti-CD109 antibody (Abcam, Cat# ab318142, 1:5000) following routine IHC procedures. Stained sections were digitally scanned, and CD109 expression was measured semi-quantitatively according to staining intensity and the percentage of positive cells.

2.4 Cell Culture, Transfection and PI3K Agonist Treatment

Human gastric tumor cell lines (HGC27, AGS, MKN45, MKN7) and immortalized gastric epithelial cells (GES1) were sourced from the Cell Bank of Type Culture Collection of the Shanghai Institute of Biochemistry and Cell Biology, Chinese Academy of Sciences (Shanghai, China). All cell lines (MKN7, HGC27, AGS, MKN45 and GES1) were cultured in RPMI-1640 medium supplemented with 10% FBS and 1% penicillin–streptomycin at 37 °C in a humidified atmosphere containing 5% CO_2. All cell lines were cultured under standardized conditions in accordance with the providers' guidelines. All cell lines were validated by short tandem repeat (STR) profiling and tested negative for mycoplasma. MKN7 and HGC27 cells were cultured in 6-well plates until they attained the requisite confluence for functional tests. The shRNA plasmids targeting CD109 and negative control empty plasmids were purchased from Tianjun Biotechnology (Guangzhou, Guangdong, China). After knockdown efficiency verification, shCD109 plasmid #2 was selected for subsequent experiments (**Supplementary Fig. 1**). The sequences were listed as follows: shCD109 (target sequence, 5′→3′): GCCGATCCTTACATAGATATT; shControl (non-targeting negative control sequence, 5′→3′): CCGGCCTAAGGTTAAGTCGCCCTCGCTCGAGCGAGGGCGACTTAACCTTAGGTTTTTG.

Lentiviruses packaged with shCD109 or shControl were separately infected into MKN7 and HGC27 cells, followed by puromycin screening to establish stable CD109-knockdown cell lines and corresponding control cell lines. Upon successful construction of stable cell strains, total RNA and cellular protein were extracted to detect the mRNA and protein expression levels of CD109 for verification of knockdown efficiency.

The PI3K agonist 740Y-P was purchased from MeilunBio (MeilunBio, Cat# MB4505, Dalian, China) and dissolved in sterile water to prepare a stock solution. For rescue experiments, cells were pretreated with the indicated treatments and then incubated with 740Y-P at a final concentration of 20 μM in complete culture medium for 24 h at 37 °C in a humidified atmosphere containing 5% CO_2. Control cells received an equal volume of vehicle (sterile water or DMSO). Following treatment, cells were harvested for subsequent assays.

2.5 Colony Formation Assay, Transwell Assays and Cell Viability Assay

For colony formation, cells were harvested 24–48 hs after transfection, resuspended to achieve a single-cell solution, and plated evenly into 6-well plates at equal seeding densities. After incubation until visible colonies (approximately ≥50 cells per colony) had developed, cells were fixed using 4% paraformaldehyde (Servicebio, Cat# G1101, Wuhan, China) and subsequently stained with 0.1% crystal violet (Servicebio, Cat# G1014, Wuhan, China). The colonies were subsequently photographed and quantified.

The migratory and invasive abilities of cells were assessed using Transwell chambers. For migration tests, transfected cells were seeded into the upper chambers using serum-free media. For invasion assays, the top surfaces of the membranes were pre-coated with Matrigel approximately 24 h prior. Following a suitable incubation period, cells that had penetrated the barrier were fixed by paraformaldehyde, stained with crystal violet, and photographed for quantitative cell enumeration.

Cell viability was assessed using the Cell Counting Kit-8 (CCK-8) assay (Servicebio, Cat# G4103, Wuhan, China) according to the manufacturer's instructions. Briefly, cells in the logarithmic growth phase were seeded into 96-well plates at a density of $1 \times 10^3 – 5 \times 10^3$ cells per well in 100 μL of complete culture medium and allowed to adhere overnight at 37 °C in a humidified atmosphere containing 5% CO_2. Following the indicated treatments, 10 μL of CCK-8 reagent was added to each well, and the plates were incubated at 37 °C for 2 h (protected from light). The absorbance was measured at 450 nm using a microplate reader. Cell viability was calculated as: Cell viability (%) = $[(As - Ab) / (Ac - Ab)] \times 100$, where As, Ac, and Ab represent the absorbance values of the sample, control, and blank (medium only) wells, respectively.

2.6 Assessment of Immunological Cell Infiltration and Functional Enrichment

The correlation between CD109 expression and the quantity of tumor-infiltrating immune cells was assessed utilizing the TISIDB database (https://cis.hku.hk/TISIDB/) [19] and the CIBERSORT deconvolution technique [20]. To clarify the putative biological functions and signaling pathways related to CD109, functional enrichment analyses were performed utilizing Gene Ontology (GO) terms and Kyoto Encyclopedia of Genes and Genomes (KEGG) pathways [21,22].

2.7 Western Blot and RT-qPCR

Total cellular protein was extracted for Western blotting using radioimmunoprecipitation assay (RIPA) lysis buffer and quantified via the bicinchoninic acid (BCA) assay. Identical quantities of protein were resolved by SDS-PAGE and subsequently transferred to polyvinyli-

Table 1. The clinicopathological characteristics related to CD109 expression in clinical sample of 120 STAD patients.

Variable	No. of patients	CD109 (High)	CD109 (Low)	*p*-value
Gender				0.152
Male	66	38	28	
Female	54	24	30	
Age (years)				0.545
<60	32	18	14	
≥60	88	44	44	
Tumor size (cm)				0.213
<5	53	24	29	
≥5	67	38	29	
Differentiation degree				0.011
Well- moderately differentiated	48	18	30	
Poorly differentiated	72	44	28	
TNM stage				0.018
I–II	45	17	28	
III–IV	75	45	30	

Table 2. Univariate and multivariate Cox proportional hazards model showing variables that affect overall survival in STAD patients (n = 120).

Variable	Univariate analysis HR (95% CI)	*p*-value	Multivariate analysis HR (95% CI)	*p*-value
Age	1.35 (1.06–1.94)	0.03	1.23 (0.84–1.56)	0.14
Gender	0.88 (0.54–1.28)	0.73	0.97 (0.76–1.47)	0.59
Stage	1.86 (1.28–2.24)	0.02	1.57 (1.15–1.96)	0.03
T	1.22 (1.01–1.78)	0.04	1.18 (1.09–1.56)	0.04
N	1.15 (1.02–1.83)	0.04	1.13 (1.04–1.72)	0.04
M	1.45 (1.14–1.97)	0.03	1.33 (1.08–1.74)	0.04
CD109	1.69 (1.26–2.03)	0.01	1.58 (1.13–1.88)	0.02

dene difluoride (PVDF) membranes. Subsequent to blocking, membranes were treated with primary antibodies targeting CD109, epithelial-mesenchymal transition (EMT) markers (N-cadherin, E-cadherin, Vimentin), and components of the PI3K/AKT pathway (p-PI3K, PI3K, p-AKT, AKT), utilizing GAPDH as a loading control. After incubation with HRP-conjugated secondary antibodies, protein bands were detected using an enhanced chemiluminescence (ECL) method. Anti-GAPDH (Abcam, Cat# ab8245, 1:10,000), anti-CD109 (Abcam, Cat# ab318142, 1:1000), anti-N-cadherin (Abcam, Cat# ab76011, 1:5000), anti-E-cadherin (Abcam, Cat# ab40772, 1:5000), anti-Vimentin (Abcam, Cat# ab92547, 1:5000), Anti-PI3K (Abcam, Cat# ab302958, 1:1000), anti-p-PI3K (Abcam, Cat# ab138364, 1:1000), anti-AKT (Abcam, Cat# ab8805, 1:2000) and anti-P-AKT (Abcam, Cat# ab38449, 1:1000) antibodies were purchased from Abcam (Cambridge, MA, USA). The secondary antibody (CST, Cat# 7076, 1:3000; CST, Cat# 7074, 1:3000) were purchased from Cell Signaling Technology (Danvers, MA, USA).

Total RNA for RT-qPCR was extracted using TRIzol reagent (Servicebio, Cat# G3013, Wuhan, China), and its concentration and purity were evaluated with a NanoDrop spectrophotometer (ND-ONE-W, Thermo Fisher Scientific, Waltham, MA, USA). cDNA was generated from pure RNA utilizing a reverse transcription kit (SMOBiO, Cat# RP1300, Beijing, China). Subsequently, quantitative PCR was conducted utilizing SYBR Green PCR Master Mix (Servicebio, Cat# G3328, Wuhan, China) on a real-time PCR apparatus. Relative mRNA expression levels were determined using the $2^{-\Delta\Delta Ct}$ technique, using GAPDH as the housekeeping gene.

2.8 Statistical Analysis

Statistical analyses were conducted with GraphPad Prism software (version 8.0, San Diego, CA, USA). Survival curves were constructed utilizing the Kaplan-Meier method, and intergroup differences were evaluated using the log-rank test. Univariate and multivariate Cox proportional hazards regression models were utilized to ascertain independent prognostic variables. Comparisons between the two groups were performed using Student's *t*-test for normally distributed data or the Mann–Whitney U test for non-normally distributed data. For the clinicopathological characteristics in Table 1, categorical variables were compared between CD109-high and CD109-low groups using

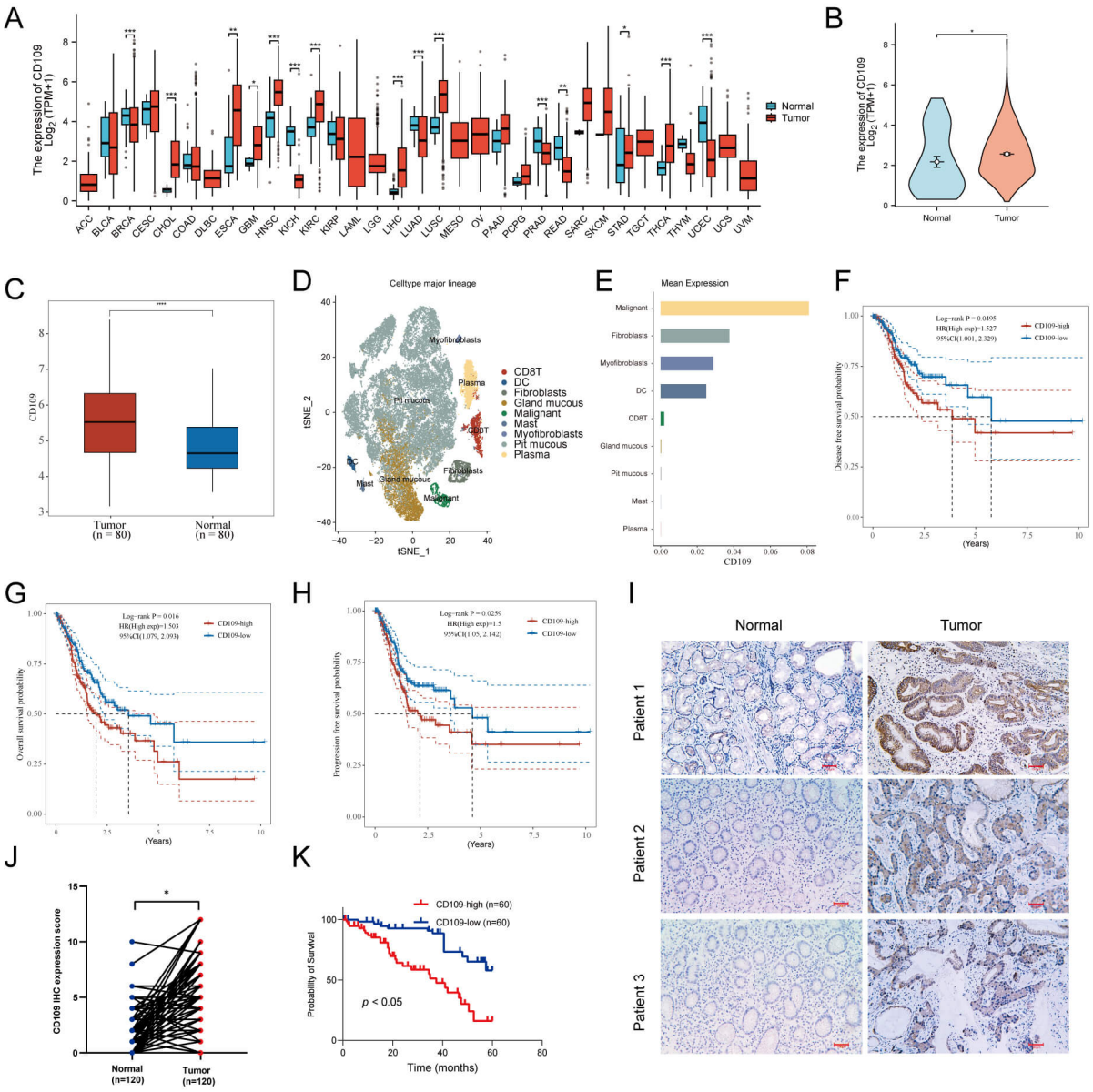


Fig. 1. Analysis of the expression level of CD109 and its association with prognosis in STAD. (A) The transcriptional profiles of *CD109* across pan-cancer tissues. (B) Differential expression analysis of *CD109* between STAD tissues and normal gastric epithelia (TCGA). (C) Comparative transcriptional analysis of *CD109* in STAD versus matched normal gastric epithelia (GEO). (D) Single-cell sequencing cell classification results. (E) *CD109* expression in different cells. (F) Kaplan-Meier survival analysis correlating *CD109* expression levels with DFS in STAD patients (TCGA). (G) Kaplan-Meier survival analysis correlating *CD109* expression levels with OS in STAD patients (TCGA). (H) Kaplan-Meier survival analysis correlating *CD109* expression levels with PFS in STAD patients (TCGA). (I) The expression of CD109 in gastric cancer tissue samples and matched normal tissues was analyzed by immunohistochemistry. Scale bar = 100 μm. (J) The blue and red dots are the immunohistochemistry scores of the tissue, and the lines between the two dots correspond to gastric cancer and paired normal tissue. (K) Kaplan-Meier survival plots delineating outcomes for STAD patients stratified by high versus low CD109 expression. (* $p < 0.05$; ** $p < 0.01$; *** $p < 0.001$; **** $p < 0.0001$). STAD, stomach adenocarcinoma; DFS, disease-free survival; OS, overall survival; PFS, progression-free survival.

the Pearson chi-square test. All *in vitro* studies were conducted in duplicate and independently repeated a minimum of three times. A *p*-value less than 0.05 was deemed statistically significant.

3. Results

3.1 Elevated CD109 Expression Correlates With Adverse Outcomes in STAD Patients

Considering the documented deregulation of CD109 in many malignancies, we initially investigated its expres-

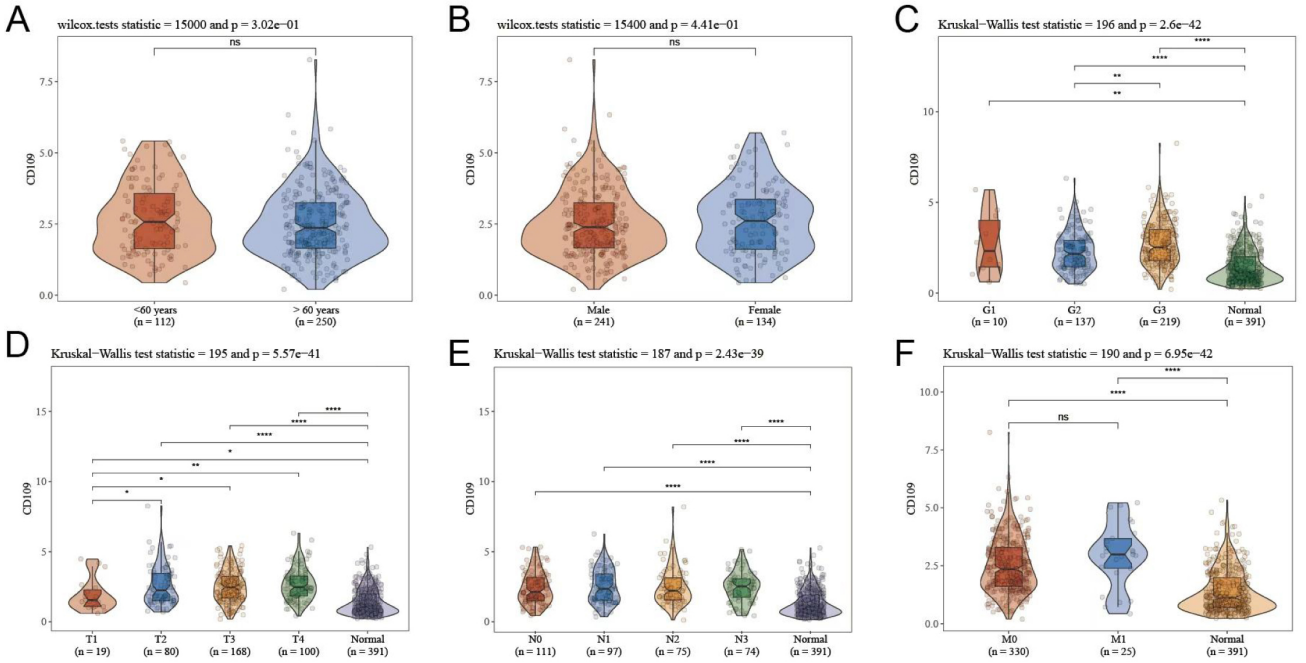


Fig. 2. Association of CD109 expression with clinicopathological features in STAD (combined TCGA-STAD and GEO cohorts). (A) Age (years). (B) Gender. (C) G stage. (D) T stage. (E) Lymph node status. (F) M stage. (ns $p > 0.05$, * $p < 0.05$; ** $p < 0.01$; **** $p < 0.0001$). The cohort analyzed in Fig. 2 is independent of the 120-patient clinical cohort presented in Table 1 and Table 2.

sion profile in STAD. Pan-cancer examination of TCGA datasets demonstrated dramatically increased CD109 mRNA levels in various cancer types, including breast cancer, cholangiocarcinoma, colorectal cancer, and particularly STAD, in comparison to adjacent normal tissues (Fig. 1A). Within the STAD cohort, CD109 expression was significantly elevated in tumor tissues compared to normal stomach tissues (Fig. 1B). Consistently, transcriptomic data retrieved from the GEO dataset (GSE27342) further validated that CD109 transcription was significantly elevated in STAD specimens (Fig. 1C). Single-cell RNA sequencing (GEO: GSE134520) findings indicated that CD109 was mostly expressed by malignant epithelial cells within the STAD microenvironment (Fig. 1D,E). Survival analysis utilizing public datasets (TCGA-STAD) indicated that individuals with elevated intratumoral CD109 expression experienced markedly reduced disease-free survival (DFS), overall survival (OS), and progression-free survival (PFS) compared to those with diminished CD109 expression (Fig. 1F–H). Clinicopathological correlation analyses indicated that CD109 levels were associated with tumor differentiation grade and T stage, among other parameters (Fig. 2A–F, Table 1). Additionally, both univariate and multivariate Cox regression analyses conducted on 120 patients with STAD identified TNM stage and CD109 expression levels as independent prognostic factors for patient outcomes (Table 2). To validate these findings, we performed immunohistochemical staining for CD109 in a cohort of 120 paired STAD and adjacent non-tumorous tissues. CD109 positivity was far more pronounced in STAD tissues compared to neighboring normal mucosa (Fig. 1I,J). In accordance with the public database findings, Kaplan-Meier analysis utilizing IHC ratings indicated that elevated CD109 expression correlated with much worse prognosis (Fig. 1K). Collectively, our data demonstrate that CD109 is commonly elevated in STAD and is significantly correlated with adverse clinical results.

3.2 CD109 Downregulation Inhibits STAD Cell Proliferation, Invasion, and Migration

To elucidate the practical function of CD109 in STAD, a series of *in vitro* functional assays were conducted. CD109 expression was initially assessed in various STAD cell lines and in normal gastric epithelial GES1 cells. Both CD109 protein and mRNA levels were markedly elevated in most cancer cell lines, with particularly high expression observed in HGC27 and MKN7 cells (Fig. 3A). Cell lines with high CD109 expression are more suitable for knockdown experiments to observe changes in functional phenotype. Consequently, these two cell types were chosen for subsequent shRNA-mediated CD109 knockdown, resulting in effective suppression of CD109 at the mRNA and protein levels (Fig. 3B). CD109 knockdown markedly attenuated the malignant characteristics of STAD cells. CCK-8 and colony formation assays revealed a pronounced reduction in cell proliferation and clonogenic capacity following CD109 knockdown (Fig. 3C,D). Furthermore, Transwell migration and invasion experiments revealed that the silencing of

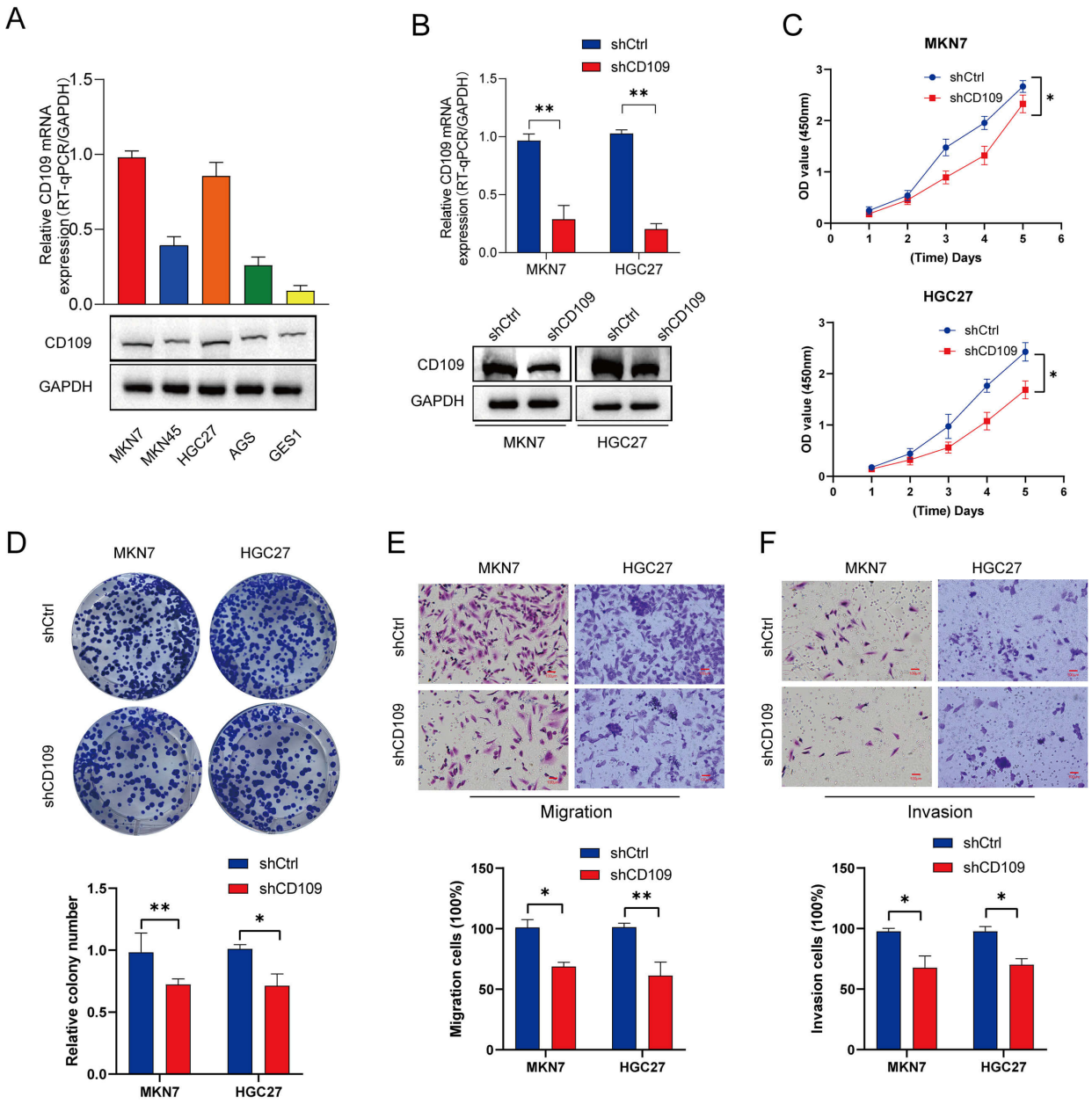


Fig. 3. CD109 regulates the proliferation, invasion, and migration abilities of STAD. (A) Comparison of mRNA (upper panel) and protein levels (lower panel) of CD109 in STAD cell lines (MKN7, MKN45, HGC27, and AGS) and normal gastric epithelial cells (GES1). Data are mean ± SD; n = 3; *t* test. (B) The CD109 knockdown STAD cell line was constructed and verified by RT-qPCR and western blot. Mean ± SD; n = 3; *t* test. (C) The effect of CD109 knockdown on the proliferation of STAD cells was analyzed by CCK-8 assay. Data are mean ± SD; n = 3; two-way ANOVA followed by Bonferroni's post hoc test. (D) Implementation of colony formation assays to quantify the influence of CD109 silencing on STAD cell proliferation. Data are mean ± SD; n = 3; *t* test. (E) Transwell assay was used to analyze the effects of CD109 knockdown on migration ability of STAD cells. Scale bar = 100 µm. Data are mean ± SD; n = 3; *t* test. (F) Transwell assay was used to analyze the effects of CD109 knockdown on invasion ability of STAD cells. Scale bar = 100 µm. Data are mean ± SD; n = 3; *t* test. (* $p < 0.05$; ** $p < 0.01$).

CD109 significantly decreased the migratory and invasive capacities of HGC27 and MKN7 cells (Fig. 3E,F). These data collectively show that CD109 enhances the proliferative, migratory, and invasive characteristics of STAD cells, affirming its function as an oncogenic driver in STAD.

3.3 CD109 Regulates the Progression of STAD via the PI3K/AKT Signaling Pathway

Having established the tumor-promoting function of CD109, we next explored the underlying molecular mechanisms. Gene set enrichment analysis (GSEA) of STAD

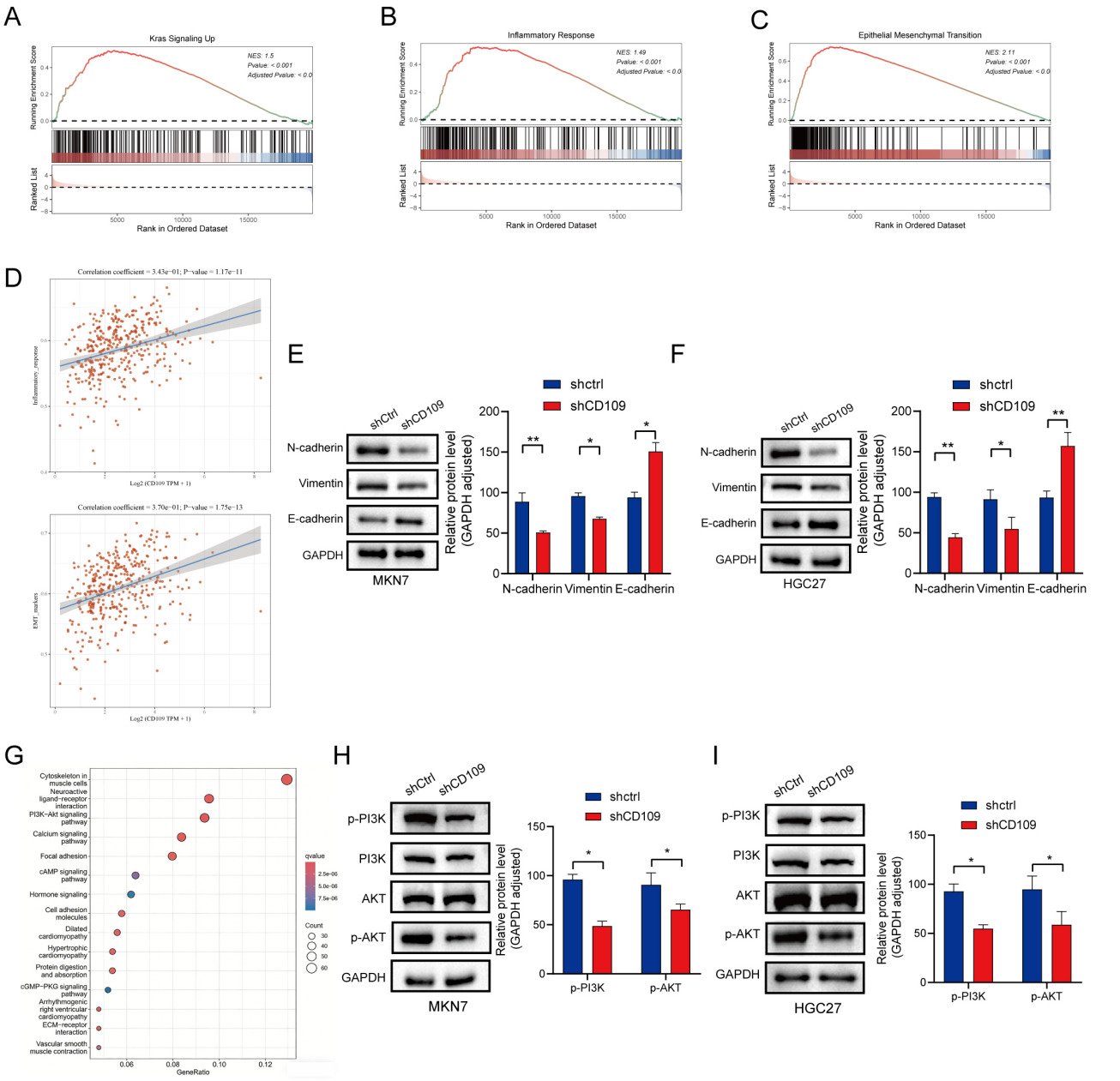


Fig. 4. CD109 regulates EMT capacity and activation of the PI3K/AKT signaling pathway in STAD. (A) Functional enrichment analysis suggests that CD109 may be involved in the regulation of the KRAS signaling pathway in STAD. (B) Functional enrichment analysis suggests that CD109 may be involved in the regulation of the inflammatory response signaling pathway in STAD. (C) Functional enrichment analysis suggests that CD109 may be involved in the regulation of the epithelial-mesenchymal transition (EMT) signaling pathway in STAD. (D) Relationship between CD109 expression and inflammatory response as well as EMT markers. (E,F) Utilization of western blotting to examine the impact of CD109 knockdown on the expression of EMT-marker proteins in STAD cells. Data are mean ± SD; n = 3; *t* test. (G) Utilizing KEGG analysis to investigate the role of CD109 in STAD. (H,I) Western blot was used to analyze the effect of CD109 knocked down on PI3K/AKT pathway. Data are mean ± SD; n = 3; *t* test. (* $p < 0.05$; ** $p < 0.01$). KRAS, Kirsten Rat Sarcoma Viral Oncogene Homolog; KEGG, Kyoto Encyclopedia of Genes and Genomes.

patient samples stratified by CD109 expression revealed significant enrichment of several cancer-related hallmark pathways in the CD109-high group, including "KRAS signaling up", "inflammatory response" and "epithelial-mesenchymal transition (EMT)" (Fig. 4A–C). Consistently, correlation analyses in the TCGA-STAD cohort showed that CD109 mRNA levels were positively associated with canonical inflammatory response genes and EMT markers (Fig. 4D). These bioinformatics findings were supported by *in vitro* experiments. Western blotting

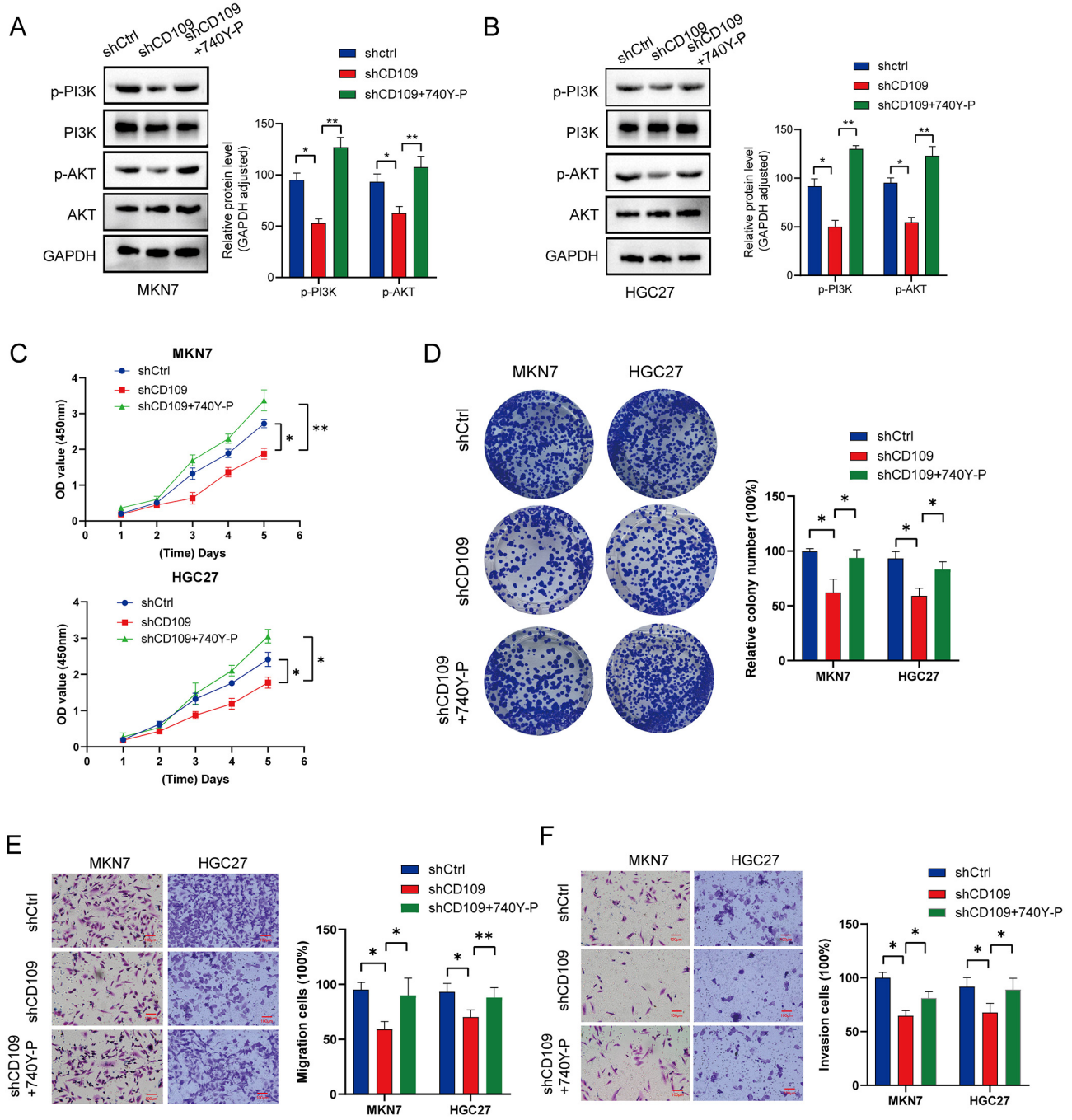


Fig. 5. The PI3K agonist 740Y-P restored the proliferation, invasion, and migration of STAD cells suppressed by CD109 down-regulation. (A) Western blotting was used to analyze the effects of CD109 knockdown and PI3K activation on the PI3K/AKT pathway in MKN7 cells. Data are mean ± SD; n = 3; one-way ANOVA followed by Tukey's post hoc test. (B) Western blotting was used to analyze the effects of CD109 knockdown and PI3K activation on the PI3K/AKT pathway in HGC27 cells. Data are mean ± SD; n = 3; one-way ANOVA followed by Tukey's post hoc test. (C) The effect of CD109 knockdown and PI3K activation on the proliferation of STAD cells was analyzed by CCK-8 assay. Data are mean ± SD; n = 3; two-way ANOVA followed by Bonferroni's post hoc test. (D) Implementation of colony formation assays to quantify the influence of CD109 silencing and PI3K activation on STAD cell proliferation. Data are mean ± SD; n = 3; one-way ANOVA followed by Tukey's post hoc test. (E) Transwell assay was used to analyze the effects of CD109 knockdown and PI3K activation on migration ability of STAD cells. Scale bar = 100 μm. Data are mean ± SD; n = 3; one-way ANOVA followed by Tukey's post hoc test. (F) Transwell assay was used to analyze the effects of CD109 knockdown and PI3K activation on invasion ability of STAD cells. Scale bar = 100 μm. Data are mean ± SD; n = 3; one-way ANOVA followed by Tukey's post hoc test. (* $p < 0.05$; ** $p < 0.01$).

revealed that CD109 knockdown in HGC27 and MKN7 cells reduced the expression of mesenchymal proteins (N-cadherin, Vimentin) while elevating the epithelial proteins E-cadherin, demonstrating the inhibition of EMT (Fig. 4E,F). KEGG pathway analysis found the "PI3K/AKT signaling pathway" as a key pathway associated with CD109 (Fig. 4G). Considering the pivotal function of PI3K/AKT in modulating cell survival, proliferation, EMT, we postulated that CD109 could influence its carcinogenic effects through this route. Consistent with this, Western blot analysis showed that CD109 knockdown significantly decreased the phosphorylation levels of PI3K and AKT, while retaining their total protein levels unchanged (Fig. 4H,I). These findings suggest that CD109 is associated with the regulation of PI3K/AKT pathway activity.

3.4 Activation of PI3K/AKT Pathway Restored the Malignant Phenotype of STAD Suppressed by CD109 Downregulation

To further demonstrate the causal relationship of the PI3K/AKT pathway in the CD109-mediated malignant phenotype of STAD, we performed a rescue experiment using the PI3K agonist 740Y-P. First, we knocked down CD109 gene expression in MKN7 and HGC27 cells using shRNA, followed by treatment with the PI3K agonist 740Y-P (20 μM, STAD cells incubated for 24 h). The results showed that the levels of PI3K/AKT phosphorylated proteins were effectively suppressed in the knockdown group, while the expression of these proteins was restored in the 740Y-P group (Fig. 5A,B). Next, we performed CCK-8 and colony formation assays, which showed that CD109 knockdown significantly reduced cell proliferation and colony formation capabilities, but the PI3K agonist restored these weakened capabilities (Fig. 5C,D). Finally, Transwell migration and invasion assays showed that 740Y-P also restored the significantly reduced tumor cell migration and invasion capabilities caused by CD109 silencing (Fig. 5E,F). These data collectively demonstrate the crucial role of the PI3K/AKT pathway in the CD109-mediated malignant phenotype of STAD.

3.5 CD109 Performs an Important Function in Modulating Infiltration of Immune Cells and Immunological Checkpoints in STAD

Previous data indicate that CD109 may modulate inflammatory responses and affect immunological status in STAD. To elucidate its immunological function, we initially examined the correlation between CD109 expression and immune cell infiltration. Analysis of the TISIDB database revealed a negative correlation between CD109 expression and $CD8^+$ T cells as well as activated $CD4^+$ T cells, while a positive correlation was observed with NKT cells (Fig. 6A–C). CIBERSORT analysis revealed that CD109 expression had a negative correlation with $CD8^+$ T cells and M1 macrophages, while indicating a positive correlation with M2 macrophages (Fig. 6D–F). To corroborate these results at the tissue level, patients were classified into high and low CD109 expression groups according to the median CD109 mRNA level. $CD8^+$ T cells and M2 macrophages were identified by IHC staining for CD8 and CD206, respectively. In accordance with the computational analysis, tumors exhibiting elevated CD109 expression showed reduced $CD8^+$ T-cell infiltration and elevated M2 macrophage infiltration (Fig. 6G), indicating an association between CD109 and an immunosuppressive tumor microenvironment.

Because our enrichment analyses implicated CD109 in inflammatory responses, we further assessed its relationship with immune regulatory molecules. TCGA-STAD data indicated that CD109 expression exhibited a positive correlation with various immunosuppressive checkpoints, including LAG3 and PDCD1LG2 (PD-L2), but negatively correlated with immunostimulatory molecules such as ENTPD1 (CD39) and LTA (Fig. 7A). We next examined broader immunological features. Patients exhibiting elevated CD109 expression showed significantly elevated tumor microenvironment (TME) ratings, encompassing stromal, immunological, and ESTIMATE scores (Fig. 7B), but exhibited lower tumor mutational burden (TMB) (Fig. 7C). Immunophenoscore (IPS) analysis, which predicts responsiveness to immune checkpoint blockade, indicated that individuals with reduced CD109 levels exhibited higher IPS values irrespective of PD-1 or CTLA-4 status (Fig. 7D–G).

These data indicate that CD109 is intricately associated with immune cell composition, fostering an immunosuppressive environment marked by diminished $CD8^+$ T-cell presence and elevated M2 macrophage infiltration, and correlates with immune checkpoint expression and immunotherapy-related scores, thereby positioning CD109 as a potential modulator of antitumor immunity and immune checkpoint regulation in STAD.

4. Discussion

STAD is frequently detected at most severe stage and is associated with dismal outcomes, highlighting the pressing need for dependable biomarkers and novel therapeutic targets [23,24]. CD109, a glycosylphosphatidylinositol-anchored surface glycoprotein, participates in multiple aspects of cellular regulation. It has been reported to facilitate tumorigenesis in several malignancies, include oral squamous cell cancer, malignant tumors, prostate carcinoma, and ovarian tumors [25,26,27,28]. Despite the documented correlation between elevated CD109 expression and adverse prognosis in STAD, the underlying processes remain inadequately elucidated.

In the present work, we systematically demonstrate the pro-tumorigenic function of CD109 in STAD. CD109 was significantly increased in both the transcript and protein levels in malignant tissues relative to adjacent non-tumorous gastric mucosa. Notably, sporadically stronger CD109 staining was also observed in a subset of nor-

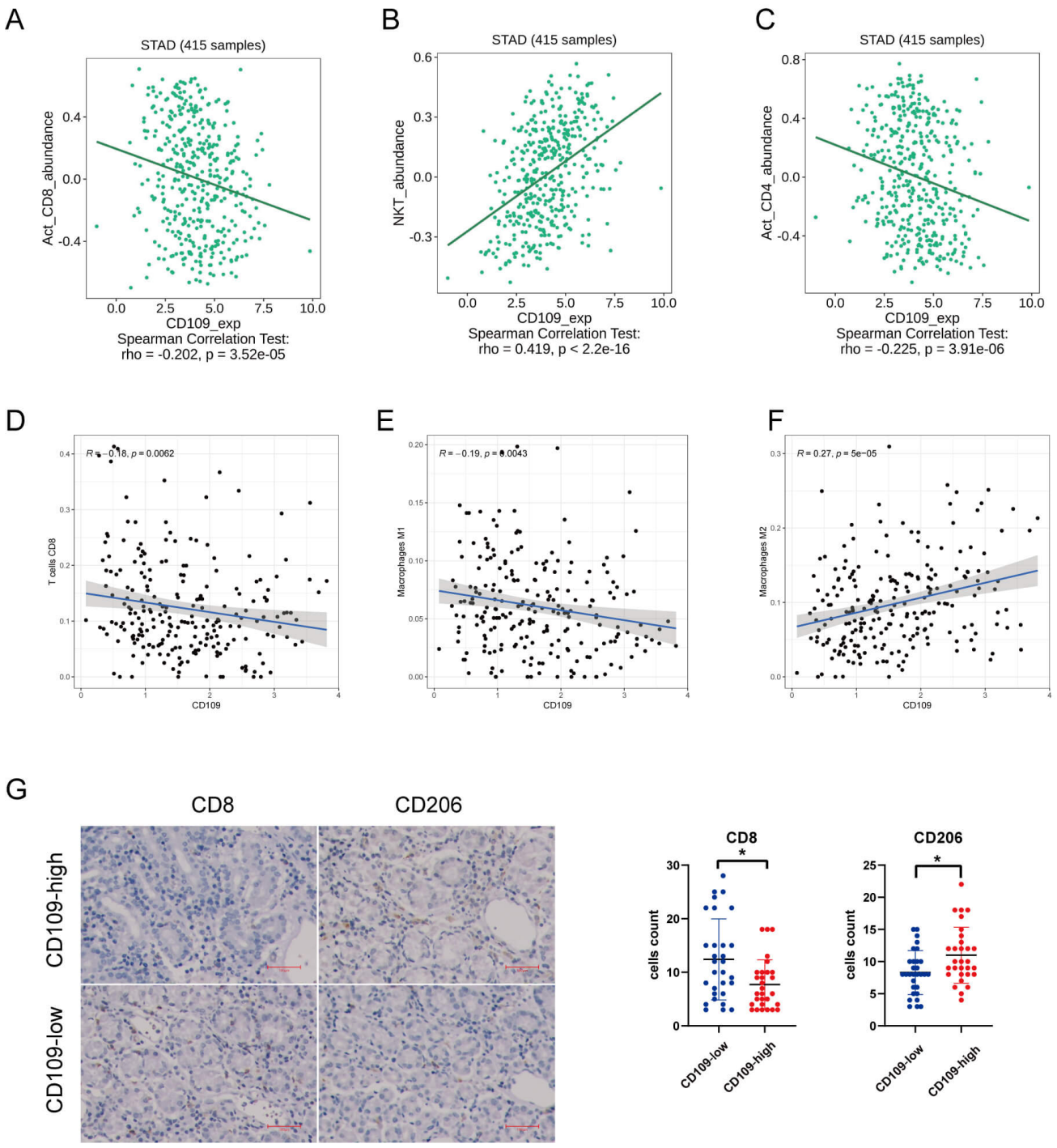


Fig. 6. The expression level of CD109 influences the immune cell infiltration abundance in STAD. (A–C) The TISIDB database was used to analyze the relationship between CD109 levels and the infiltration abundance of various immune cells. (D–F) CIBERSORT algorithm was used to evaluate the association of CD109 with diverse immune cells. (G) Immunohistochemistry was utilized to analyze the relationship between CD109 expression levels and the infiltration of $CD8^+$ T cells and M2 macrophages in STAD tissues. Scale bar = 100 μm. Data are mean ± SD; n = 30 for CD109_low_Exp group and n = 30 for CD109_high_Exp group; *t* test. (* $p < 0.05$).

mal gastric glands, a pattern that could likewise be detected in certain paired samples from public cohorts. This phenomenon may reflect context-dependent regulation of CD109 and the substantial heterogeneity of gastric epithelium and gastric cancers, where individual genes may exert distinct or even contrasting roles in different cellular settings. Significantly, investigations of public databases and our clinical cohort repeatedly demonstrated that elevated CD109 expression is highly correlated with decreased overall survival in individuals with STAD.

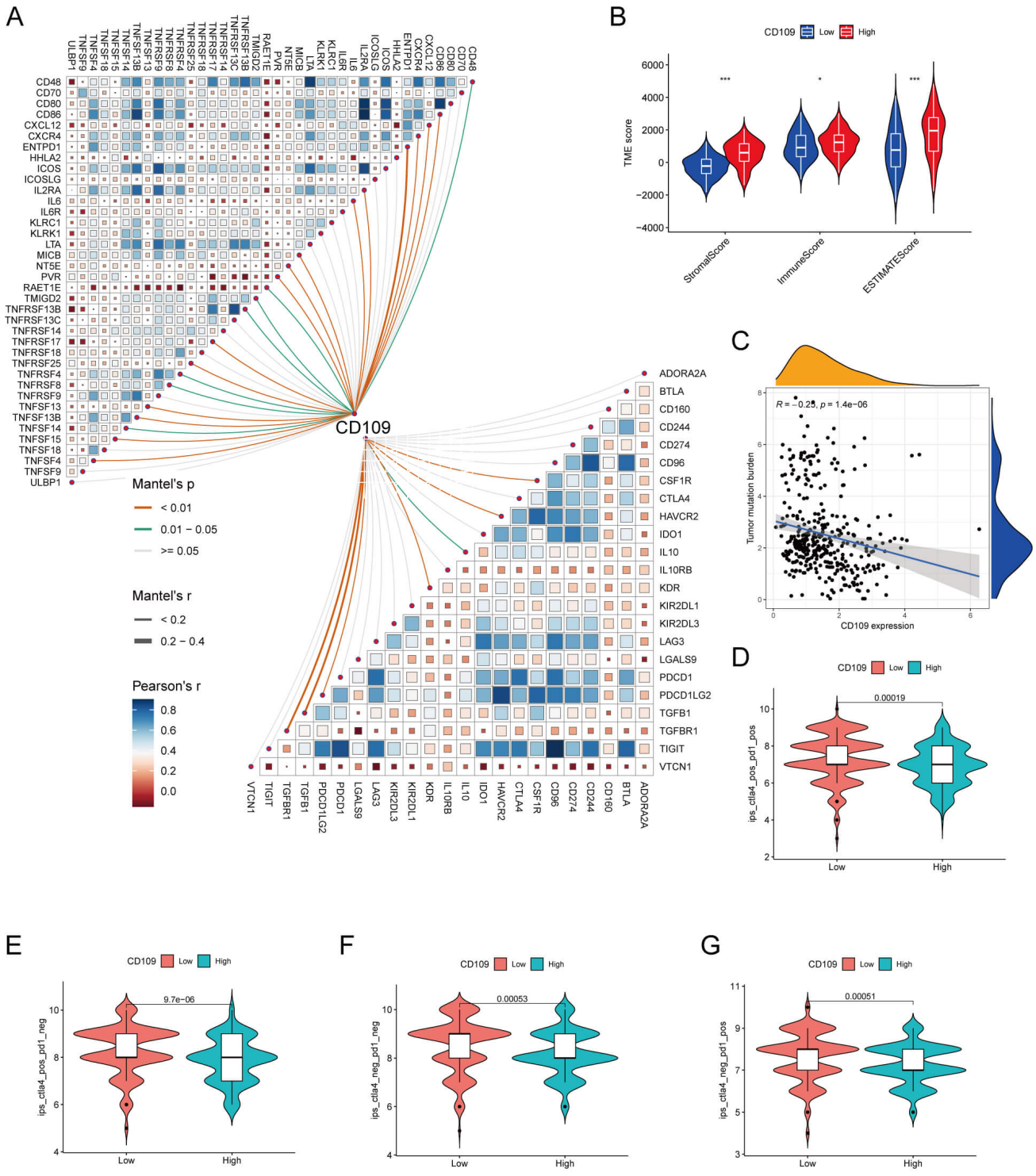


Fig. 7. The expression of immune checkpoint molecules is closely associated with the level of CD109. (A) Correlation analysis of CD109 with the expression levels of immune inhibitor and immune stimulator. (B) Correlation analysis between CD109 expression levels and TME score. (C) Analysis of the correlation between CD109 expression levels and TMB in STAD. (D) Patients with low CD109 expression have higher IPS scores when both CTLA4 and PD1 are positive. (E) Patients with low CD109 expression levels have higher IPS scores when CTLA4 is positive and PD1 is negative. (F) Patients with low CD109 expression exhibit higher IPS scores when CTLA4 is negative and PD1 is positive. (G) Patients with low CD109 expression attain higher IPS scores when both CTLA4 and PD1 are negative. (* $p < 0.05$; *** $p < 0.001$).

Although TNM classification remains the standard tool for prognostic assessment in STAD, our univariate Cox analysis identified CD109 expression, together with age and T/N/M stages, as significant prognostic variables. In multivariate Cox regression analysis, both CD109 expression and TNM-related variables (T, N, and M categories) remained statistically significant, indicating that CD109 expression is an independent prognostic factor in addition to conventional TNM staging in this cohort. However, because of relatively small sample size and individual-center design of the present investigation, necessitating validation in larger, multi-center cohorts.

GSEA indicated that increased CD109 expression correlates with the enrichment of EMT signatures. EMT is pivotal processes driving metastatic dissemination and tumor maintenance. Consistently, *in vitro* assays showed that silencing CD109 partially reversed EMT-associated marker changes and impaired the migratory and invasive capability of STAD cells. Subsequent pathway analysis revealed that signaling pathways such as PI3K/AKT are key downstream effectors. The PI3K/AKT pathway is one of the core oncogenic pathways regulating cell survival, proliferation, EMT. In gastric cancer, its abnormal activation has been widely confirmed to drive malignant tumor progression [29,30]. KEGG analysis showed that the PI3K/AKT pathway was significantly enriched in the CD109 high-expression group, and this pathway has a clear biological association with known TGF-β and JAK-STAT signaling crosstalk of CD109 [31,32]. As a central transducer of the phosphoinositide 3-kinase (PI3K) signaling axis, Akt regulates key cellular processes such as growth, proliferation, apoptosis, survival, and migration in both normal and cancer cells, and its dysregulation is a hallmark of many malignancies [33]. Although the cytoskeleton regulation and ligand-receptor interaction pathways were enriched at a high rate, their direct evidence in CD109-mediated tumor progression was relatively limited. Therefore, we chose the PI3K/AKT pathway, which has a clearer mechanism and stronger verifiability, as the priority for validation. The decrease in PI3K and AKT phosphorylation following CD109 knockdown, together with the well-established role of PI3K/AKT signaling in controlling EMT and tumor progression, supports a working model in which CD109 promotes an aggressive STAD phenotype through modulation of the PI3K/AKT axis. A key limitation is that the origin of this regulatory mechanism remains unclear, and future studies are needed to elucidate it.

Beyond its cell-intrinsic effects, our data suggest that CD109 also contributes to shaping the immune microenvironment of STAD. We observed an inverse correlation between CD109 expression and infiltration of cytotoxic $CD8^+$ T cells—the principal mediators of anti-tumor immunity—and a positive correlation with M2-polarized macrophages, which are widely recognized for their roles in tumor promotion and immunosuppression [34,35]. These bioinformatic findings were corroborated by IHC analysis in patient specimens. Moreover, the strong associations between CD109 and multiple immune checkpoint molecules raise the possibility that CD109 may modulate responsiveness to immune checkpoint inhibitors (ICIs). The molecular mechanisms by which CD109 affects immune-cell recruitment, functional polarization, and checkpoint regulation, however, remain to be elucidated and constitute an important focus for subsequent research.

5. Limitations

This work offers new insights into the oncogenic function of CD109 in stomach adenocarcinoma (STAD), although numerous limitations must be recognized when interpreting our results.

Initially, all functional investigations were performed solely *in vitro* with gastric cancer cell lines. While our findings consistently indicate that CD109 knockdown inhibits proliferation, migration, invasion, and EMT *in vitro*, the lack of *in vivo* animal models—such as xenograft, orthotopic, or immunocompetent tumor models—restricts our capacity to confirm the tumor-promoting and immune-modulatory roles of CD109 in a physiological setting. Thus, the translational significance of our findings on tumor growth and metastasis in living creatures has yet to be determined.

The clinical dataset employed for prognostic analysis is confined to 120 patients from a single institution, and the prognostic significance of CD109 has not been corroborated in independent public cohorts, including those from GEO or ACRG. Consequently, larger multi-center prospective cohorts are necessary to validate the generalizability of our results.

Notwithstanding these constraints, our research offers a thorough and comprehensive analysis of CD109 in STAD, integrating bioinformatics, clinical tissue validation, and functional tests. The aforementioned limitations do not diminish the primary conclusions but instead emphasize significant avenues for future research.

6. Conclusion

In summary, this study systematically integrates TCGA big data analysis, single-cell sequencing data mining, clinical tissue validation, and *in vitro* functional tests, thoroughly elucidating the expression characteristics, prognostic significance, and functional mechanisms of CD109 in STAD. Studies have shown that CD109 knockdown reduces p-PI3K and p-AKT levels, whereas the PI3K agonist 740Y-P partially restores these phosphorylation levels. These results support a role for CD109 in regulating PI3K/AKT pathway activity. This study systematically elucidates the correlation between CD109 expression and the reduction of $CD8^+$ T cell infiltration, the augmentation of M2 macrophage infiltration, and the expression of immune checkpoint molecules within the STAD immune microen-

vironment, indicating that CD109 may function as a potential biomarker for forecasting immunotherapy response. Collectively, these findings support CD109 as both a clinically relevant prognostic indicator and an attractive therapeutic target in STAD. Future investigations should aim to dissect the precise mechanisms by which CD109 regulates anti-tumor immunity and to assess CD109-directed interventions in appropriate preclinical models.

Availability of Data and Materials

The datasets produced and examined in this investigation are accessible from the corresponding author upon a reasonable request. The public data utilized in this investigation are detailed in the Materials and Methods section.

Author Contributions

Conceptualization, Writing - original draft and Writing - review & editing: YYang, YW, CZ, YYan, YF and KZ; Data curation, Formal analysis, Investigation and Methodology and Project administration: YYang, YW, CZ, YYan, YF; Resources: YYang, KZ; Software, Supervision, Validation and Visualization: YYang, KZ; All authors made substantial contributions to the article and granted approval for its submission. All authors read and approved the final manuscript. All authors have participated sufficiently in the work and agreed to be accountable for all aspects of the work.

Ethics Approval and Consent to Participate

This study was executed in complete adherence to the principles of the Declaration of Helsinki, ensuring compliance with ethical norms and the legal stipulations of the host country. This study has been approved by the Ethics Committee of the First Affiliated Hospital of Jinan University (KY-2023-120). All patients signed informed consent forms.

Acknowledgment

Not applicable.

Funding

This research received no external funding.

Conflicts of Interest

The authors declare no conflicts of interest.

Supplementary Material

Supplementary material associated with this article can be found, in the online version, at https://doi.org/10.31083/FBL52984.

References

[1] Bray F, Laversanne M, Sung H, Ferlay J, Siegel RL, Soerjomataram I, et al. Global cancer statistics 2022: GLOBOCAN estimates of incidence and mortality worldwide for 36 cancers in 185 countries. CA: A Cancer Journal for Clinicians. 2024; 74: 229–263. https://doi.org/10.3322/caac.21834

[2] Thrift AP, El-Serag HB. Burden of Gastric Cancer. Clinical Gastroenterology and Hepatology: the Official Clinical Practice Journal of the American Gastroenterological Association. 2020; 18: 534–542. https://doi.org/10.1016/j.cgh.2019.07.045

[3] Morgan DR, Corral JE, Li D, Montgomery EA, Riquelme A, Kim JJ, et al. ACG Clinical Guideline: Diagnosis and Management of Gastric Premalignant Conditions. The American Journal of Gastroenterology. 2025; 120: 709–737. https://doi.org/10.14309/ajg.0000000000003350

[4] Mourato MB, Pratas N, Branco Pereira A, Chança R, Fronteira I, Dinis R, et al. Effectiveness of Gastric Cancer Endoscopic Screening in Intermediate-Risk Countries-A Systematic Review and Meta-Analysis. United European Gastroenterology Journal. 2025; 13: 1715–1729. https://doi.org/10.1002/ueg2.70084

[5] Joshi SS, Badgwell BD. Current treatment and recent progress in gastric cancer. CA: a Cancer Journal for Clinicians. 2021; 71: 264–279. https://doi.org/10.3322/caac.21657

[6] Dang HH, Ta HDK, Nguyen TTT, Anuraga G, Wang CY, Lee KH, et al. Prospective role and immunotherapeutic targets of sideroflexin protein family in lung adenocarcinoma: evidence from bioinformatics validation. Functional & Integrative Genomics. 2022; 22: 1057–1072. https://doi.org/10.1007/s10142-022-00883-3

[7] Tran TO, Lam LHT, Le NQK. Hyper-methylation of ABCG1 as an epigenetics biomarker in non-small cell lung cancer. Functional & Integrative Genomics. 2023; 23: 256. https://doi.org/10.1007/s10142-023-01185-y

[8] Yoon HH, Jin Z, Kour O, Kankeu Fonkoua LA, Shitara K, Gibson MK, et al. Association of PD-L1 Expression and Other Variables With Benefit From Immune Checkpoint Inhibition in Advanced Gastroesophageal Cancer: Systematic Review and Meta-analysis of 17 Phase 3 Randomized Clinical Trials. JAMA Oncology. 2022; 8: 1456–1465. https://doi.org/10.1001/jamaoncol.2022.3707

[9] Wang Y, Chong G. Immunotherapy in gastric adenocarcinoma - a rapidly evolving treatment landscape. Critical Reviews in Oncology/Hematology. 2025; 216: 104941. https://doi.org/10.1016/j.critrevonc.2025.104941

[10] Elewaut A, Estivill G, Bayerl F, Castillon L, Novatchkova M, Pottendorfer E, et al. Cancer cells impair monocyte-mediated T cell stimulation to evade immunity. Nature. 2025; 637: 716–725. https://doi.org/10.1038/s41586-024-08257-4

[11] Lee SH, Lee D, Choi J, Oh HJ, Ham IH, Ryu D, et al. Spatial dissection of tumour microenvironments in gastric cancers reveals the immunosuppressive crosstalk between CCL2+ fibroblasts and STAT3-activated macrophages. Gut. 2025; 74: 714–727. https://doi.org/10.1136/gutjnl-2024-332901

[12] Cui T, Sun L, Guo X, Cheng C, Zhang N, Zhou S, et al. Tumor-derived CD109 orchestrates reprogramming of tumor-associated macrophages to dampen immune response. Journal of Hepatology. 2025; 83: 946–958. https://doi.org/10.1016/j.jhep.2025.03.035

[13] Tanabe M, Hosokawa K, Nguyen MAT, Nakagawa N, Maruyama K, Tsuji N, et al. The GPI-anchored protein CD109 protects hematopoietic progenitor cells from undergoing erythroid differentiation induced by TGF-β. Leukemia. 2022; 36: 847–855. https://doi.org/10.1038/s41375-021-01463-3

[14] Batal A, Garousi S, Finnson KW, Philip A. CD109, a master regulator of inflammatory responses. Frontiers in Immunology. 2025; 15: 1505008. https://doi.org/10.3389/fimmu.2024.1505008

[15] Yoo HB, Moon JW, Kim HR, Lee HS, Miyabayashi K, Park CH, et al. A TEAD2-Driven Endothelial-Like Program Shapes

Basal-Like Differentiation and Metastasis of Pancreatic Cancer. Gastroenterology. 2023; 165: 133–148.e17. https://doi.org/10.1053/j.gastro.2023.02.049

[16] Mii S, Enomoto A, Shiraki Y, Taki T, Murakumo Y, Takahashi M, et al. CD109: a multifunctional GPI-anchored protein with key roles in tumor progression and physiological homeostasis. Pathology International. 2019; 69: 249–259. https://doi.org/10.1111/pin.12798

[17] Zhang D, Luo Y, Lin Y, Fang Z, Zheng H, An M, et al. Endosomal Trafficking Bypassed by the RAB5B-CD109 Interplay Promotes Axonogenesis in KRAS-Mutant Pancreatic Cancer. Advanced Science (Weinheim, Baden-Wurttemberg, Germany). 2024; 11: e2405092. https://doi.org/10.1002/advs.202405092

[18] Wu WT, Li YJ, Feng AZ, Li L, Huang T, Xu AD, et al. Data mining in clinical big data: the frequently used databases, steps, and methodological models. Military Medical Research. 2021; 8: 44. https://doi.org/10.1186/s40779-021-00338-z

[19] Li L, Wang F, Deng Z, Zhang G, Zhu L, Zhao Z, et al. DCLRE1B promotes tumor progression and predicts immunotherapy response through METTL3-mediated m6A modification in pancreatic cancer. BMC Cancer. 2023; 23: 1073. https://doi.org/10.1186/s12885-023-11524-8

[20] Zhang S, Wan X, Lv M, Li C, Chu Q, Wang G. TMEM92 acts as an immune-resistance and prognostic marker in pancreatic cancer from the perspective of predictive, preventive, and personalized medicine. The EPMA Journal. 2022; 13: 519–534. https://doi.org/10.1007/s13167-022-00287-0

[21] Denny P, Feuermann M, Hill DP, Lovering RC, Plun-Favreau H, Roncaglia P. Exploring autophagy with Gene Ontology. Autophagy. 2018; 14: 419–436. https://doi.org/10.1080/15548627.2017.1415189

[22] Ogata H, Goto S, Sato K, Fujibuchi W, Bono H, Kanehisa M. KEGG: Kyoto Encyclopedia of Genes and Genomes. Nucleic Acids Research. 1999; 27: 29–34. https://doi.org/10.1093/nar/27.1.29

[23] Tian Y, Qiu S, Yang S, Jiang Y, Hu H, Yang C, et al. The oncogenic role and prognostic value of PXDN in human stomach adenocarcinoma. BMC Cancer. 2024; 24: 1463. https://doi.org/10.1186/s12885-024-13097-6

[24] Feng X, Shi T, Wei J. Translational advances in gastric cancer: integrating biomarkers, novel therapies, and microenvironment remodeling in 2025. Translational Cancer Research. 2026; 15: 218. https://doi.org/10.21037/tcr-2025-1-2812

[25] Hassan A, Kungyal T, Zhou S, Blati M, Finnson K, Bertos N, et al. IL-6-mediated tumorigenicity and antioxidant state in squamous cell carcinoma cells are driven by CD109 via stabilization of IL-6 receptor-alpha and activation of STAT3/NRF2 pathway. Experimental Hematology & Oncology. 2025; 14: 64. https://doi.org/10.1186/s40164-025-00630-x

[26] Solé C, Tramonti D, Schramm M, Goicoechea I, Armesto M, Hernandez LI, et al. The Circulating Transcriptome as a Source of Biomarkers for Melanoma. Cancers. 2019; 11: 70. https://doi.org/10.3390/cancers11010070

[27] Mitra Ghosh T, Mazumder S, Davis J, Yadav J, Akinpelu A, Alnaim A, et al. Metronomic Administration of Topotecan Alone and in Combination with Docetaxel Inhibits Epithelial-mesenchymal Transition in Aggressive Variant Prostate Cancers. Cancer Research Communications. 2023; 3: 1286–1311. https://doi.org/10.1158/2767-9764.CRC-22-0427

[28] Kim JS, Shin MJ, Lee SY, Kim DK, Choi KU, Suh DS, et al. CD109 Promotes Drug Resistance in A2780 Ovarian Cancer Cells by Regulating the STAT3-NOTCH1 Signaling Axis. International Journal of Molecular Sciences. 2023; 24: 10306. https://doi.org/10.3390/ijms241210306

[29] Khoshdel F, Mottaghi-Dastjerdi N, Yazdani F, Salehi S, Ghorbani A, Montazeri H, et al. CTGF, FN1, IL-6, THBS1, and WISP1 genes and PI3K-Akt signaling pathway as prognostic and therapeutic targets in gastric cancer identified by gene network modeling. Discover Oncology. 2024; 15: 344. https://doi.org/10.1007/s12672-024-01225-4

[30] Morgos DT, Stefani C, Miricescu D, Greabu M, Stanciu S, Nica S, et al. Targeting PI3K/AKT/mTOR and MAPK Signaling Pathways in Gastric Cancer. International Journal of Molecular Sciences. 2024; 25: 1848. https://doi.org/10.3390/ijms25031848

[31] Mulliqi E, Khelwatty S, Bagwan I, Kamaludin A, Morgan A, Long N, et al. The Co-Expression and Cellular Location of HER Family Members, EGFRvIII, Putative Cancer Stem Cell Biomarkers CD44 and CD109 in Patients with Glioblastoma, and Their Impacts on Prognosis. Cancers. 2025; 17: 1221. https://doi.org/10.3390/cancers17071221

[32] Bizet AA, Tran-Khanh N, Saksena A, Liu K, Buschmann MD, Philip A. CD109-mediated degradation of TGF-β receptors and inhibition of TGF-β responses involve regulation of SMAD7 and Smurf2 localization and function. Journal of Cellular Biochemistry. 2012; 113: 238–246. https://doi.org/10.1002/jcb.23349

[33] Leiphrakpam PD, Batra R, Tenner L, Are C. Targeting Akt signaling pathway in cancer: molecular mechanisms and advances in therapeutic interventions. Frontiers in Bioscience-Landmark. 2025; 30: 39100. https://doi.org/10.31083/FBL39100

[34] Meiser P, Knolle MA, Hirschberger A, de Almeida GP, Bayerl F, Lacher S, et al. A distinct stimulatory cDC1 subpopulation amplifies CD8+ T cell responses in tumors for protective anticancer immunity. Cancer Cell. 2023; 41: 1498–1515.e10. https://doi.org/10.1016/j.ccell.2023.06.008

[35] Chen S, Saeed AFUH, Liu Q, Jiang Q, Xu H, Xiao GG, et al. Macrophages in immunoregulation and therapeutics. Signal Transduction and Targeted Therapy. 2023; 8: 207. https://doi.org/10.1038/s41392-023-01452-1